

# Evaluating Fairness and Mitigating Bias in Machine Learning: A Novel Technique using Tensor Data and Bayesian Regression

**Kuniko Paxton**

K.AZUMA-2021@HULL.AC.UK

*School of Computer Science and DAIM  
University of Hull  
Hull, East Riding of Yorkshire, HU6 7RX, UK*

**Koorosh Aslansefat**

K.ASLANSEFAT@HULL.AC.UK

*School of Computer Science  
University of Hull  
Hull, East Riding of Yorkshire, HU6 7RX, UKA*

**Dhavalkumar Thakker**

D.THAKKER@HULL.AC.UK

*School of Computer Science and DAIM  
University of Hull  
Hull, East Riding of Yorkshire, HU6 7RX, UK*

**Yiannis Papadopoulos**

Y.I.PAPADOPOULOS@HULL.AC.UK

*School of Computer Science and DAIM  
University of Hull  
Hull, East Riding of Yorkshire, HU6 7RX, UK*

**Editor:** My editor

## Abstract

Fairness is a critical component of Trustworthy AI. In this paper, we focus on Machine Learning (ML) and the performance of model predictions when dealing with skin color. Unlike other sensitive attributes, the nature of skin color differs significantly. In computer vision, skin color is represented as tensor data rather than categorical values or single numerical points. However, much of the research on fairness across sensitive groups has focused on categorical features such as gender and race. This paper introduces a new technique for evaluating fairness in ML for image classification tasks, specifically without the use of annotation. To address the limitations of prior work, we handle tensor data, like skin color, without classifying it rigidly. Instead, we convert it into probability distributions and apply statistical distance measures. This novel approach allows us to capture fine-grained nuances in fairness both within and across what would traditionally be considered distinct groups. Additionally, we propose an innovative training method to mitigate the latent biases present in conventional skin tone categorization. This method leverages color distance estimates calculated through Bayesian regression with polynomial functions, ensuring a more nuanced and equitable treatment of skin color in ML models.

**Keywords:** Fairness, Skin Color, Skin Lesion Classification, Statistical Distance

## 1 Introduction

Advanced Deep Learning (DL) is gaining widespread use across various domains, potentially influencing society profoundly. Accordingly, attention has turned towards the risks associated with DL. A significant risk to consider is unfairness towards protected characteristics, such as race, gender, age and ethnicity. In this manuscript, we define explanatory variables associated with those protected characteristics as Sensitive Attributes (SAs). Against this background, research on fairness has dramatically increased and achieved a certain level of success. Most of the research has focused on Group Fairness (GF). GF pertains to ensuring that arbitrary evaluation metrics, such as accuracy, approximate similar ratios across all groups derived from SAs Ruggieri et al. (2023). Fairness is inherently a comparative and contested concept Jacobs and Wallach (2021) that necessitates grouping. In this context, and consistent with its legal significance, GF exerts broad social influence. Prioritizing GF in legal terms is essential for achieving the generalization needed to eliminate illegal discrimination and enhance social equality Xiang and Raji (2019). On the other hand, there are also warnings against focusing on optimizing average performance in classification tasks Ruggieri et al. (2023) as there is a possibility that hidden unfairness may exist within groups deemed fair by GF definitions. To solve this problem, the concept of individual fairness was introduced. Individual fairness emphasizes individual fairness that is not dependent on groups, based on the principle that "similar individuals should be treated similarly" Dwork et al. (2012). However, in prior research, while the importance of IF has been acknowledged, there have been fewer studies that explicitly quantify individual discrimination. Some argue that IF serves as an auxiliary concept and cannot define fairness from legal, social, moral, and non-shareable perspectives (Binns, 2020). Nevertheless, IF should also be protected and should not be optional to improve the fairness and safety usage of DL. That is why the fairness framework needs a definition to certify IF within the same group that achieved GF.

Fairness in ML contains two important aspects: its protected characteristics and target units. The protected characteristics are characteristics of individuals that should not be discriminated against by-laws or guidelines, such as gender and race. In this manuscript, we define data elements of protected characteristics as sensitive attributes to distinguish them clearly. The sensitive attributes are categorized into three types. We defined them below.

- Categorical sensitive attribute: Most of the protected characteristics have this type of attribute. The sensitive attribute  $a$  is an element of a set of arbitrary encoded numbers. Each element is a discrete value that does not have any relationship with the numbers themselves. For example, giving a sensitive attribute  $a$  is gender can only take one of the categorical values in the defined set  $\{0 : \text{male}, 1 : \text{female}\}$ .
- Single numeric sensitive attribute: Age and income are examples of this type, and the data is one of continuous numeric values, such as  $a = \{1, \dots, N\}$ .
- Dimensional sensitive attribute: This is the attribute that cannot be represented as either a categorical sensitive attribute or a single numeric sensitive attribute, for example, tensor,  $a \in \{x | x \sim (h, w, c)\}$  where  $h, w, c$  are height, width, color channel, and vector data,  $a \in \{x | x \sim (n)\}$  where  $n$  is a vector.

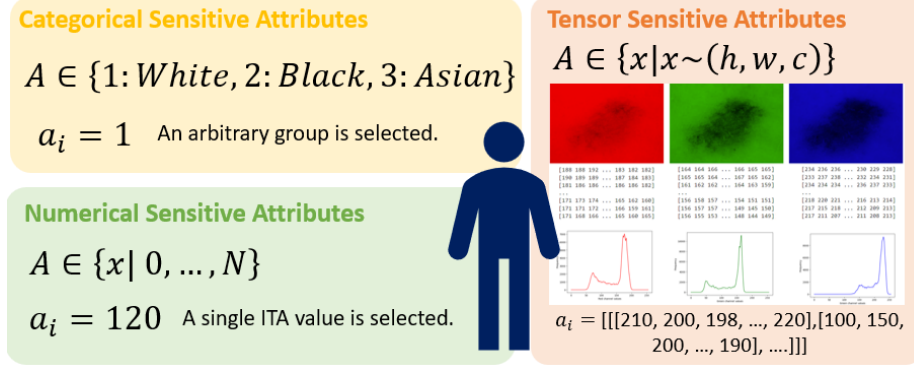


Figure 1: Difference of Sensitive Attributes

The reason GF predomination up to today is the data characteristics of the SA. Many SAs are categorical values. Many SAs are categorical values. For example, giving SA  $a$  is gender can only take one of the categorical values in the defined set  $\{\text{male}, \text{female}\}$ . This can be selected using judgment based on well-defined criteria, such as biological gender. These categorical values fit with GF definitions often used in fairness studies, such as Equal Opportunity Hardt et al. (2016), Equalized Odds Hardt et al. (2016), and Demographic Parity Zafar et al. (2017). Equal opportunity is defined as the ratio of predicted label  $\hat{Y} = 1$  to true label  $Y = 1$  in one group (e.g., male) is equal to or less than a certain threshold compared to the ratio in another group (e.g., female). Specifically, the condition of Eq.1 needs to be satisfied,

$$P_{\text{privileged}}(\hat{Y} = 1 | A = \text{male}, Y = 1) \approx P_{\text{protected}}(\hat{Y} = 1 | A = \text{female}, Y = 1) \quad (1)$$

It is relatively easy to apply this fairness definition because GF directly refers to SA,  $A$ , (e.g., gender) when calculating the predicted probability. On the other hand, when  $A$  is not categorical values, such as income, age or skin color, it becomes difficult to directly apply the same conditions. In such cases, it is necessary to either appropriately group the continuous values or take a different approach. Another type of protected attribute, such as age, takes single numerical data, for example,  $a = \{1, \dots, N\}$ . Such attributes are given a single data value in tabular data or annotations. For example, Mary et al. (2019); Grari et al. (2019); Giuliani et al. (2023); Lee et al. (2022) measured fairness by verifying independence using the Hirschfeld-Gebelein-Rény even when the observed data points are numerical values in the case of the regression tasks. Brotto et al. (2024) et al. assumed that the prediction includes bias when there is a correlation between the input variable and the numerical value of the SA, which is endogenous. The numerical SA was divided into intervals, and it was judged to be fair when the minimum value of the loss was within the threshold of fairness that was allowed by Oneto et al. (2020) et al. These methods use single numerical values for individual data observations. These can reflect individual characteristics better than categorization. These methods use density intervals and mini-batches to communicate with the fairness definitions, such as equal opportunity. However, there are complex cases where these methods cannot sufficiently reflect individual characteristics. For example, in

the case of skin color, the data is tensor,  $a \in \{x|x \sim (h, w, c)\}$  where  $h$ ,  $w$ ,  $c$  are height, width, color channel, in computer vision. For example, individuals categorized as "white" exhibit a wide range of phenotypic diversity, and reducing them to a single racial category may be problematic from the fairness perspective. Capturing this diversity is difficult using simple categorization. These examples highlight the demand for approaches that address fairness at the individual level, even within the same group. In the following subsection, we investigate the complexities of skin color and review how these SAs have been treated in previous studies.

### 1.1 Skin Colour in Deep Learning Classification

A particular case of this risk is unfairness in the predictive performance of DL image classification models, e.g. for cancer detection, depending on skin color Lin et al. (2024); Muthukumar (2019); Buolamwini and Gebru (2018); Bevan and Atapour-Abarghouei (2022); Pakzad et al. (2022); Sarridis et al. (2023). Prior studies have contributed to the consensus that ML classifiers perform poorly on darker skin tones and better on lighter skin tones. Skin color is a well-recognized protected characteristic that should not be discriminated against under emerging guidelines legislation.gov.uk (2013) on AI safety. Skin color is one of the difficult sensitive attributes to address in research of AI fairness. There are two key difficulties.

The first is the difficulty in achieving consistency in objective judgments of skin color. Experts have not achieved complete agreement on skin color grouping in previous studies Groh et al. (2022); Krishnapriya et al. (2021); Heldreth et al. (2024). There are numerous skin color scales Thong et al. (2023), such as the Fitzpatrick (1988) validity and Monk skin scales Schumann et al. (2024), but there is still no established method for identifying a single definitive skin color categorization. Moreover, the grouping of skin color is not determined exclusively by its color. It is frequently substituted for ethnic groups, such as Black, White and Asian. While race is classified according to physical characteristics, ethnicity is determined by an individual's background Bulatao and Anderson (2004). Considering the increase in diversity in modern society, the racial characteristics of traditional ethnic groups can not necessarily be represented. Research indicated that individuals selected their ethnicity, taking into account the context. Therefore, whether an individual's skin color is light or dark is a subjective judgment, and there is the possibility that biases caused by category selection may be hidden.

However, these studies focus on simple tabular numerical data, and such data is intrinsically different from image data Tian et al. (2022). Skin color does not fit easily into studied these categories. Skin color is tensor data,  $a \in \{x|x \sim (h, w, c)\}$  where  $h$ ,  $w$ ,  $c$  are height, width, color channel, in computer vision and is represented as the set of each pixel in the skin area, represented with values for each of the three primary colors. Nevertheless, most previous research on ML biases on skin color has assumed traditional group classification. The differences between the same group are fundamentally ignored Chouldechova and Roth (2018). Categorization involves and amplifies the risk of uncertainty by statistically averaging Ruggieri et al. (2023).

Furthermore, large parts of research demand skin color type annotation on image data. This requires a great deal of effort and annotation accuracy is critical Kalb et al. (2023). A classification method that included skin color differences without annotations was proposed,

but this was based on transfer learning, and annotations were still used for the source model Hwang et al. (2020). To our knowledge, no research has achieved a fair model without annotations using only detected skin color nuances. The primary factor contributing to bias is the imbalance in the distribution of skin tones in available datasets. Hence, several studies also focus on creating balanced datasets Gustafson et al. (2023); Karkkainen and Joo (2021).

Motivated by the above, we propose a method for measuring skin color to assess individual fairness for skin color within and across subgroups. Unlike previous methods, this method converts skin pixels tensor data to a probability distribution. It then uses a statistical distance to measure the differences in the probability distribution of each individual’s skin color while maintaining the gradation and color nuances of the skin. The method enables the detection of skin color bias that has previously been masked within groups, and the identification of biases that have not been detected due to the lack of annotations. Furthermore, we propose a method of weighting the loss function by the distance to mitigate the bias detected by our method. This method reduces the correlation between skin color distribution and performance.

## 2 Related Work

We focus on image classification focusing on skin color that affects fairness towards racial or ethnic groups. Generative image, facial recognition, and object segmentation tasks are out of the scope. Earlier studies have shown that bias arises from the limited number of images available for darker skin tones. **Generative Adversarial Networks (GAN)** have therefore been used to balance the dataset by oversampling images with minority skin tones Rezk et al. (2022). Another method was to generate counterfactual data of minority skin tones Li and Abd-Almageed (2022); Dash et al. (2022). These methods generally require the same effort as creating balanced datasets. Another approach to the detection of skin cancer with ML is **Removal or Compliment**. The method removed sensitive attributes. Chiu et al. (2024) proposed a technique for skin lesion classification that classifies the type of disease based only on features related to the target attributes and does not distinguish features associated with the sensitive attribute, which is skin color. A method was proposed for clinical skin image data that takes into account differences in skin tone and aligns with the text data and with the Masked Graph Optimal Transport subsequently denoised Gaddey et al. (2024). Lee et al. (2021) et al. proposed selective classification. These methods succeed in specific datasets and conditions, but they cannot apply to general skin datasets. Other relevant research focused on the application of **Explainability techniques**. Wu et al. (2022) performed saliency calculations and reduced disparities between groups by averaging out the importance of the parameters for each skin-color group. Cross-Layer Mutual Attention Learning mitigated bias by complementing the features of deep layers with the color features found in shallow layers Manzoor and Rattani (2024). These methods compared the differences between groups of features that the model focused on during the prediction process and ignored the disparities in skin color between individuals. **Adversarial learning** separates the sensitive attributes during learning to prevent the model from learning sensitive attribute features Li et al. (2021); Du et al. (2022); Park et al. (2022); Wang et al. (2022); Bevan and Atapour-Abarghouei (2022). In an application for Deep Fake detection,

demographic information, including protected attributes and fake features, was separately trained and merged to optimize the loss Lin et al. (2024). All of these methods tend to result in relatively complex model structures. **Fairness-constrained and Reweighting learning** was applied with a weighted loss function using weighted cross-entropy to mitigate bias Hänel et al. (2022). Our bias mitigation technique is also categorized into this concept, but the reweighting methodology is fundamentally different. Ju et al. (2024) et al. have proposed a demographic-agnostic Fair Deepfake Detection that minimizes the error for the worst performance by group creating a new loss function to guarantee fairness even when annotations for sensitive attribute groups are missing. Lin et al. (2022) proposed a method for balancing the importance of weights within a model for subgroups in the pruning process. Thong and Snoek (2021) et al. used a latent vector space to remove the bias from the image. Another approach developed Q-learning in reinforcement learning to minimize bias by setting rewards according to the skewness in class distance between races Wang and Deng (2020). A bias removal by converting an image into a sketch kept the features for the model decision Yao et al. (2022). Zhang et al. (2022) et al. proposed a fairness trigger to add biased information to images. By clarifying the edge of the skin lesions, the difference in accuracy between light-skinned and dark-skinned samples was eliminated Yuan et al. (2022). In the implementation of fair image classification for skin tones, various algorithms, such as those mentioned above, have been proposed. Nevertheless, there is a commonality among all these studies that they categorize or assume grouping skin tone. Therefore, potential biases may still remain in those mitigation systems. The finer characteristics of skin should be taken into account. To address these challenges with the existing fairness evaluation and unfairness mitigation approach, we propose a new statistical-based approach and weighted loss function learning with the following main contributions:

1. In the context of skin color image classification tasks, we propose an innovative algorithm to evaluate more nuanced individual fairness within group fairness without annotation and by using statistical distance and Bayesian regression.
2. We demonstrate the ability to uncover latent bias within categorization using our method.
3. We propose a new training method to mitigate latent bias across the spectrum of skin color variation, creating a new weighted loss function by weight cross-entropy.
4. We evaluate the effectiveness of the training method in mitigating latent bias.

### 3 Methodology

#### 3.1 Fairness Definition

As mentioned in the introduction, it is difficult to accurately capture the diverse and sensitive attributes of a group using simple categorization. In order to respond to diversification and to consider fairness at the individual level, even within the same group, we extend the traditional group fairness definitions to accommodate continuous sensitive attributes by incorporating the statistical distance. Here, we explain using Equal Opportunity and Wasserstein Distance.

### 3.1.1 BACKGROUND

The Equal Opportunity criterion Hardt et al. (2016) ensures that the true positive rates are equal across different groups defined by a sensitive attribute  $A$ . For a binary sensitive attribute, the fairness constraint is expressed as:

$$P\left(\hat{Y} = 1 \mid A = 0, Y = 1\right) = P\left(\hat{Y} = 1 \mid A = 1, Y = 1\right), \quad (2)$$

where  $\hat{Y}$  is the predicted label and  $Y$  is the true label.

### 3.1.2 EXTENSION TO CONTINUOUS SENSITIVE ATTRIBUTES

When  $A$  is continuous (e.g., skin tone measured on a continuous scale), Equation (2) is not directly applicable. To address this, we introduce a distance metric that quantifies the difference between different values of  $A$  and a reference point  $A_0$  (e.g., the lightest skin tone). We use the Wasserstein Distance to measure this difference.

### 3.1.3 WASSERSTEIN DISTANCE WITH DIRECTIONAL SIGNIFICANCE

Let  $\mathcal{F}(A)$  denote the cumulative distribution function (CDF) of the sensitive attribute  $A$ . The Wasserstein Distance between two values  $A_0$  and  $A_i$  is defined as:

$$\mathcal{D}(A_0, A_i) = \int_{-\infty}^{\infty} |\mathcal{F}(A_0) - \mathcal{F}(A_i)| dA \cdot \text{sign}(A_i - A_0), \quad (3)$$

where  $\text{sign}(A_i - A_0)$  captures the direction of the difference, indicating whether  $A_i$  is greater than or less than  $A_0$ .

### 3.1.4 REWRITING THE EQUAL OPPORTUNITY CONSTRAINT

We adjust the Equal Opportunity constraint to incorporate the continuous nature of  $A$  and the distance metric:

$$\int_{-\infty}^{\infty} \mathcal{D}(A_0, A) \left[ P\left(\hat{Y} = 1 \mid A, Y = 1\right) - P\left(\hat{Y} = 1 \mid A_0, Y = 1\right) \right] dF_{A|Y=1}(A) = 0. \quad (4)$$

where  $dF_{A|Y=1}(A)$  is the probability density function of  $A$  given  $Y = 1$ .

### 3.1.5 INTERPRETATION

Equation (4) ensures that the weighted difference in true positive rates between any value of  $A$  and the reference point  $A_0$  integrates to zero over the distribution of  $A$  given  $Y = 1$ . The weighting by  $\mathcal{D}(A_0, A)$  accounts for both the magnitude and direction of the difference in the sensitive attribute.

## 3.2 Fairness Measuring and Mitigating Bias

Figure 2 illustrates the learning method for the proposed bias mitigation. This learning method is divided into two processes. The first process is the prior learning process, which

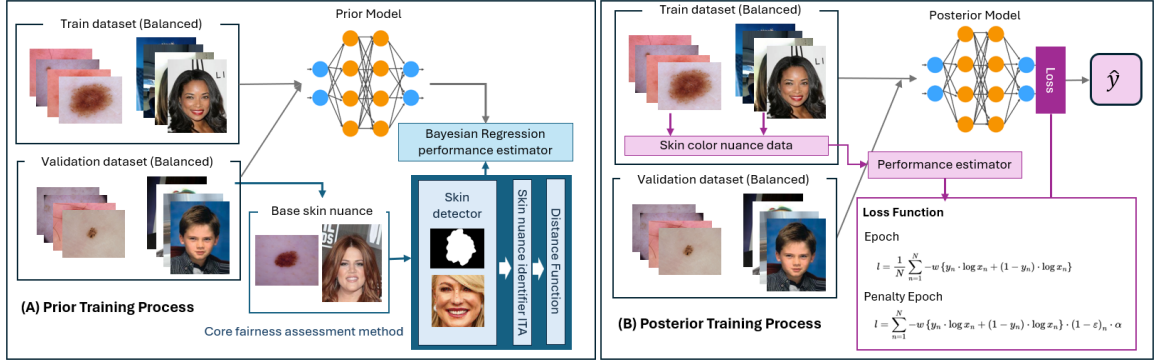


Figure 2: Bias Mitigation Learning Process: The performance estimator for the posterior training is a Bayesian regression created in the prior training phase. In the posterior training, the skin color of the training data is measured. The base skin color is the same as the validation data. One of two types of loss functions is applied depending on the epoch.

includes general training and skin color measures. An image from each dataset is selected as the baseline skin color distribution for validation, as the validation performance is used as prior data for Bayesian regression. Then, the distance between the color differences of all other validation data is measured from the baseline color. The process of measuring skin color is explained in detail in the following subsections. A performance estimator model is created by fitting the results and validation predictions using Bayesian regression. This estimator is assembled during the second process, known as posterior training. The posterior training applies a weighted loss function that penalizes the inverse of predictive distance performance.

### 3.3 Skin Color Identifier

Our method aims to preserve the nuances of pigmentation inherent in skin tones. In computer vision, skin color in color images comprises three pigments across three channels per pixel. In our study, to align with human perception for real-world applicability and enable direct comparison with categorical skin types used in previous research, we adopt the Individual Typology Angle (ITA). ITA is frequently used for skin color fairness studies as the foundation of representative skin colors Kinyanjui et al. (2019); Corbin and Marques (2023); Kalb et al. (2023); Mohamed et al. (2023). However, these studies treat ITA values as a single numerical value, representing a single continuous numeric sensitive attribute group. In extant research the nuances of skin tone pixels are not considered; instead, they are averaged out. Furthermore, even the ITA values themselves are not retained to measure fairness; they are replaced with categorical values. This results in disregarding the inherent properties of skin color. ITA is calculated in the CIELab color space according to the following equation for ITA in algorithm 1.  $L$  and  $b$  are defined as Lightness and b-hue.



$$ITA = \frac{\arctan\left(\frac{L-50}{b}\right) \times 180}{\pi} \quad (5)$$

---

**Algorithm 1** Skin Colour Identifier: Creating Skin Nuance Color Distribution

---

**Input:** Image  $x \in \mathbb{R}^{w \cdot h \cdot 3}$ 
**Output:** Nuance ITA Skin Colour Distribution  $ita$ 

```

1: Extract skin pixels:  $S = SkinDetector(x)$  {Selected based on the dataset type.}
2: Convert to CIELab color space:  $L, A, B = CIELab(S)$ 
3: Initialize nuance distribution:  $ita$ 
4: for each pixel( $i, j$ ) in  $x$  do
5:   Get luminance:  $l = L_{i,j}$ 
6:   Get blue-yellow component:  $b = B_{i,j}$ 
7:   if  $l \neq 0$  and  $b \neq 0$  then
8:     Compute ITA score:  $ITA(l, b)$  using Eq.5 and Append to  $ita$ 
9:   end if
10: end for
11: return  $ita$ 

```

---

### 3.3.1 MEASURING SKIN COLOUR DISTANCE

Assuming the distributions are IID, the Wasserstein Distance (WD) is recognized as one of the best approaches for capturing changes in the geometry of the distribution, effectively highlighting shifts that reflect underlying data transformations Cai and Lim (2022). Optimal Transport, such as WD, is a popular approach to fairness. However, those research studies concentrated to categorical sensitive attributes. For example, in the research by Chiappa and Pacchiano (2021), Optimal Transport was used to verify fairness; however, the primary purpose was to compare the continuous distribution of predicted scores rather than the distribution of input values. We measure the variability of skin color shades across images using WD. Specifically, the baseline image, denoted by  $x_0$ , is selected randomly from the validation dataset, serving as the reference distribution. Subsequent distributions, represented by  $x_i$  where  $i$  indexes these distributions, are compared against  $x_0$  using the Wasserstein metric Eq.3. This metric assesses the extent to which the skin color distributions shift towards lighter or darker tones, assigning a quantitative measure that reflects the minimal cost of transport from the baseline to each observed distribution. The sign function,  $\mathcal{S}(x_0, x_i)$  is defined by following Eq.6. Then, the values measured by WD are multiplied by the sign to quantify the difference between skin tones and their saturation direction.

$$Sign = \mathcal{S}(x_0, x_i) = \begin{cases} -1 & : median(x_0) \geq median(x_i) \\ 1 & : median(x_0) < median(x_i) \end{cases} \quad (6)$$

At this point in the process, each individual's data is converted into a one-dimensional vector. The distribution is created by a probability density function by vector values. This distribution by probability density function represents the individual's nuanced, sensitive attributes. This distribution varies from one data set to another. The differences in this

distribution, so to speak, between probability distributions of individual characteristics are measured by the Washer Stain Distance method. Specifically, we first select one sample data. The difference between the probability distribution of vector values of this sample data and the probability distribution of vector values of other data is measured by the Washer Stain Distance. The measured distance will be a single number that expresses the differences in individual characteristics relative to the base data.

### 3.4 Performance Estimation Bayesian Regression Model

Since our techniques are designed for binary classification, where individual predictions are either 0 or 1, performance cannot be effectively measured at the individual level. To address this, batches are created by small groups of similar distances after sorting in ascending order of the  $\mathcal{D}(x_0, x_i)$ . The batch size was set to 1% of the validation dataset, allowing for a more accurate assessment of performance in the experiment. The technique uses Bayesian Regression to predict performance using generic models from skin tones. Let  $D = \{d_0, \dots, d_{n-1}\}^T$  denote the vector representing the distance from baseline skin color as measured by the distance function above. The performance associated with distance is  $M = \{m_0, \dots, m_{n-1}\}$  where  $n$  is the number of instances. The visualization of the observed performance suggests that the regression model assumed polynomial features. The degree of the polynomial regression depends on the model and dataset and is determined from the prior distribution. The degree denotes  $g$ .

$$D = \begin{bmatrix} d_0 & d_0^2 & \dots & d_0^{g-1} \\ d_1 & d_1^2 & \dots & d_1^{g-1} \\ \vdots & \vdots & \ddots & \vdots \\ d_{n-1} & d_{n-1}^2 & \dots & d_{n-1}^{g-1} \end{bmatrix} \quad (7)$$

The prior distribution  $p(M|D, w, \alpha)$ , follows the Gaussian Distribution,  $\mathcal{N}(M|D_w^g, \alpha^{-1})$ .  $w$ , and  $\alpha^{-1}$  are, respectively, the coefficients and the precision. The coefficients  $w$  are provided by Spherical Gaussian:  $p(w|\lambda) = \mathcal{N}(\mu, \lambda^{-1}I_p)$ , where  $\mu$  is mean and set 0. Given the distance  $D_{test} = \{d_0, \dots, d_{n-1}\}^T$  of the new test data  $X_{test}$ , the likelihood of the prediction performance  $\hat{M}_{test} = \{m_0, \dots, m_{n-1}\}$  is calculated  $\mathcal{P}(m|d)$  using the following equation.

$$\hat{M}_{test} = \mathbb{E}[m] = \int m p(m|p) dm \quad (8)$$

In this process, we identify the bias caused by individual differences in sensitive attributes in order to understand the degree of re-weighting. For this reason, we will train using a general model that does not take fairness into account. We will call this general model the base model. We will use a Bayesian regression model to understand the relationship between the results of training this base model and the distance measured in the previous process. We will use the performance of the evaluation metric that we want to guarantee a certain level of fairness for as the input value for the Bayesian regression in this case. We can use something like equal opportunity, for example, as well as accuracy.

### 3.5 Latent Bias Mitigation

The binary cross entropy loss function is used to guide bias mitigation. The individual loss  $l$  is formulated as follows. The penalty value assigned to the binary cross entropy loss is calculated by weighting and averaging the prediction performance inversion using the softmax function,

$$\sigma(1 - \varepsilon)_i = \frac{e^{(1-\varepsilon)_i}}{\sum_{j=1}^K e^{(1-\varepsilon)_j}}, \quad (9)$$

where  $(1 - \varepsilon)$  denotes the penalty, and  $\varepsilon$  is performance prediction calculated based on skin color probability distribution distance by the Bayesian Regression Estimator equation. Since the convolutional neural network-based model gradually focuses on more detailed features in the learning process, it is unnecessary to penalize the nuanced features of the skin in the early stages of learning. Therefore, only the binary cross-entropy value is applied until the middle of the process, and weighting is performed after that.  $\alpha$  is a penalty weight. The entire Loss function is algorithm 2.

The aim of this process is to minimize the re-weighted loss. First, if it is a binomial distribution, we use binary cross-entropy, and if it is a multinomial distribution, we use cross-entropy.

$$l_n = -w \{y_n \cdot \log x_n + (1 - y_n) \cdot \log x_n\} \cdot \sigma \cdot \alpha \quad (10)$$

---

**Algorithm 2** Distance Loss Function: Calculate loss function with distance penalty

---

**Input:** Prediction  $\hat{y}$ , Target Label  $y$ , Distance  $d$ , Penalty Epoch  $pe$ , Epoch  $e$ , Batch size  $N$

**Output:** Loss  $l$

```

1: Initialize:  $BCE_{total} = 0$ 
2: for each  $y$  and  $\hat{y}$  in batch ( $n = 1$  to  $N$ ) do
3:   Compute binary cross-entropy:  $BCE_n = \text{BinaryCrossEntropy}(\text{Sigmoid}(\hat{y}), y)$ 
4:   Accumulate loss:  $BCE_{total} += BCE_n$ 
5: end for
6: if  $e \leq pe$  then
7:   Compute average loss:  $l = BCE_{total}/N$ 
8: else
9:   Compute fairness adjustment:  $\varepsilon = \text{BayesianPerformanceEstimator}(d)$ 
10:  Compute penalty weight:  $p = \text{Softmax}(1 - \varepsilon)$ 
11:  Apply penalty:  $l = \sum_{n=1}^N BCE_n \cdot p_n \cdot \alpha$ 
12: end if
13: return loss  $l$ 
```

---

## 4 Experimental Setup: Datasets and Models

### 4.1 Datasets

We selected the following three datasets. In the medical domain, Human Against Machine with 10000 training images (HAM) Tschandl et al. (2018, 2020) was one of the popular

datasets used in skin lesion classification. CelebFaces Attributes Dataset (CelebA): Liu et al. (2015), and UTKFace Zhang et al. (2017) were selected in the human face field. UTKFace dataset was chosen because skin tones are often categorized by ethnic group. Race is sometimes used to contextualize or identify with skin color Barrett et al. (2023). Each dataset was divided into a training set (60%), a validation set (20%), and a test set (20%). The imbalanced data causes bias against the minority group. Therefore, resampling is used to balance the groups with sensitive attributes, and in recent years, data from minority groups has been generated using cGAN, autoencoders, and class-based defusion models. The result is to make the number of images between groups the same or similar. Following the ideas, we fabricated a state where **group fairness has been achieved** using the following method.

**Group fairness achieved conditions.**

1. The targeting labels were balanced in training, validation, and test datasets.
2. The majority of the skin color types were employed in training, validation, and test datasets.

The detailed breakdown of the datasets is shown in the table in the appendix. Different approaches were employed to detect skin depending on the dataset because the background conditions for skin pixels differ. The details are shown in Table 1.

## 4.2 Skin Lesion Image Preprocessing

In our experiment, we performed skin lesion segmentation (SLS) and hair removal methods by Morphological Transformations (MT) to mask elements other than skin color. To fit our dataset, we conducted the following steps by OpenCV in the hair removal process. Images read with grayscale were removed noise with the opening before the black-hat. Then, hair areas were enhanced with Histogram Equalisation (CLAHE) and hair was removed by thresholding. The kernel sizes, grid sizes, clip limits, and thresholds were heuristics based on the visual perspective of each dataset. Our MT approach is well-known in the hair removal or hair inpainting process Suiçmez et al. (2023); Lee et al. (1997); Jaworek-Korjakowska and Tadeusiewicz (2013). The HAM dataset provides segmentation data.

## 4.3 Human Face Image Preprocessing

For the human face-related datasets, which are CelebA and UTKFace, we applied the facial recognition landmark method to detect skin pixels using Dlib Library King (2009). The non-face areas, including the eyes and above the top of the eyes and mouth, were then masked. Images for which face recognition was not possible, such as side view of faces, were excluded.

## 4.4 Models

A total of five models were experimented with, three of which were Convolutional Neural Network-based models and two of which were transformed-based models. Three pre-trained models using the ImageNet dataset, Very Deep Convolutional Networks (VGG16) Simonyan and Zisserman (2014), EfficientNet7B (EffNet) Tan and Le (2019), and ResNet50 He et al.

Table 1: Experiment dataset

Dataset	UTKFace	CelebA	HAM	ISIC2024
Tasks	Gender	Face attribute	Skin lesion	Skin lesion
Category	Ethnic Group	Not Pale	Skin Type 1	Skin Type 1
Preprocess	Landmark	Landmark	MT and SLS	MT and SLS
Target	Male	Positive	Melanoma	Melanoma
Train (n)	7133	6426	1300	
Validation (n)	2348	2134	434	
Test (n)	2348	2129	434	

(2016), were selected for this experiment. All are based on convolutional networks and are commonly used in image classification tasks. Since the data set was undersampled to create balanced subcategories, reducing the number of available images for training, pre-trained models were incorporated. This approach ensures that good performance can still be achieved, even with a limited amount of training data. Each model was additionally trained for each dataset. The general performance and training conditions are shown in Table 4 below. As can be seen from Table 4, the general prediction results demonstrated that the models did not differ significantly in performance based on skin color tone.

#### 4.5 Selecting Performance Evaluation Metrics

Our technique detects and mitigates the latent bias caused by individual skin tone categorization. It focuses on ensuring individual fairness using the skin tone spectrums. Therefore, we do not evaluate our technique on group-level fairness metrics such as Demographic Parity Zafar et al. (2017), Equalised Odds, and Equal Opportunity Hardt et al. (2016), which are commonly used in studies that categorize skin tones directly. Since our model is mitigating bias on an individual level, it’s important to reduce both false positives (cases where an individual’s skin tone is misclassified) and false negatives (where bias is not detected). The F1 score provides a balanced view of both types of errors, especially useful when classes (or skin tones) are imbalanced, which can easily happen in skin tone data. Consequently, the F1 score and Accuracy are selected as the evaluation metrics to focus on. The proposed mathematical formulations of concepts for Equal Opportunity, Demographic Parity, and Equalized Odds for continuous attributes are given in Section 3.1, Appendix B.1 and B.2.

## 5 Results

In this section, we describe the results of the experiment. Figure 3 illustrates the ten samples extracted from the UTKFACE dataset. All of these samples are face images annotated as ‘white’ skin color. Image (A) shows the original image with added landmarks in red. Image (B) shows the skin area in the face extracted by the landmarks, with the non-skin color areas masked in black. From these images, it is evident that the skin color gradation differs from each face when viewed by human eyes. Figure (C) plots the probability distribution of the pixels of only the skin color area of (B). In this figure, the visual nuance differences of the image in (B) can be expressed numerically.

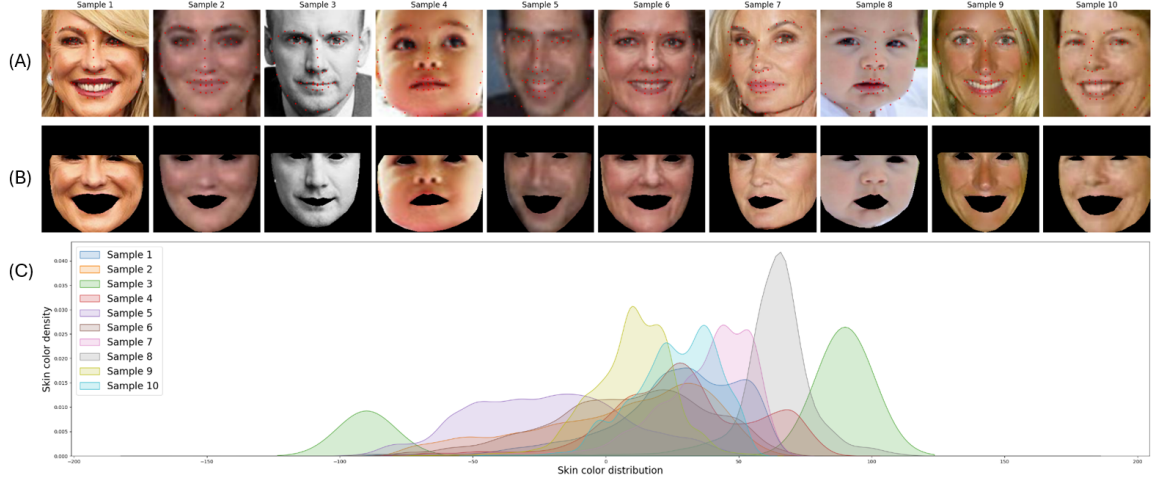


Figure 3: Examples for skin gradation distribution: (A) These are the original image and the landmark of the 10 UTKFACE samples. (B) These are images in which only the skin pixels have been extracted by masking out all pixels except for the skin pixels. (C) is a probability distribution of the ITA values calculated for each skin pixel.

Figure 4 is a performance prediction Bayesian regression model fitted using the validation data as a prior and general model. The blue plots employed the F1 score as the metric, and the green plots show Accuracy. The red horizontal line shows the mean score for the validation dataset. The grey scatter plot provides the prior observed data. The value on the X-axis is 0 for the base sample. The lighter skin colors are the larger values, and the darker are the greater negative values. In the case of the weaker correlation between skin color and performance, the Bayesian regression performance estimator, such as CelebA, is flatter. Conversely, UTKFace and HAM tend to have apparent differences depending on skin color. This shows that the element of skin color has an enormous impact on the model’s predictions. The observed individuals of predictions that are below the average of the prior are due to their skin spectrum. Next, the results of the posterior training process of incorporating the model that predicts the change in F1 score according to the skin tone displayed in Figure 4 into the loss function are shown in Table 2. Table 3 shows the correlation between the performance of each evaluation metric and distance when the batch size is 1%. In the prior training, a negative correlation with the F1 score was shown in the UTKFace and HAM datasets. The performance deteriorated as the color gradient became lighter. In the HAM dataset, a correlation was also observed in the Eff and ResNet accuracy. In the CelebA dataset, no correlation was provided in any of the models. This is because the skin color in this dataset was centered around the median compared to the others.

The results of the posterior-training bias mitigation are shown on the right side of Table 3. In most cases of the combination of the models and datasets, the correlations

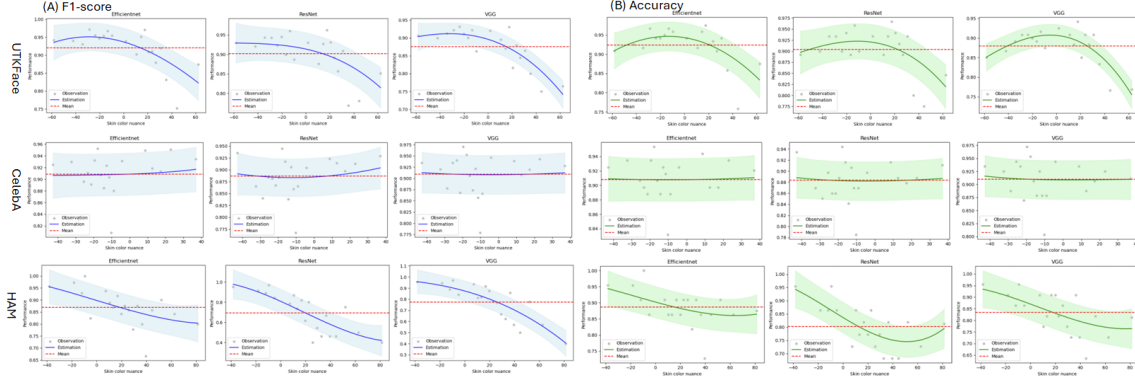


Figure 4: Bayesian Performance Estimators: This shows the performance prediction of the Bayesian regression model using the validation dataset as prior for each model and dataset. The blue graph (A) is a prediction model based on the F1 score, and the green graph (B) is based on accuracy.

Table 2: Posterior training performance results

Dataset	UTKFace			CelebA			HAM		
Model	Eff	ResNet	VGG	Eff	ResNet	VGG	Eff	ResNet	VGG
lr	1e-5	1e-5	1e-6	1e-6	1e-6	1e-6	1e-5	1e-5	1e-6
Epochs	23	23	19	29	28	24	23	19	12
Penalty Start	16	17	1	17	17	17	12	18	15
Penalty Weight	0.95	1	0.95	1	1	1	0.95	0.95	1
Val F1	0.89	0.91	0.88	0.91	0.88	0.92	0.90	0.87	0.81
Val ACC	0.89	0.91	0.88	0.91	0.88	0.92	0.90	0.87	0.81
Test F1	0.89	0.91	0.88	0.90	0.87	0.90	0.90	0.85	0.81
Test ACC	0.89	0.91	0.88	0.90	0.87	0.90	0.90	0.85	0.81

between distance F1 score and accuracy were mitigated. The CelebA, which originally showed no correlation, also had relatively decreased coefficients. In the case of the UTKFace dataset and models of Efficientnet and Resnet, the weak correlation was no longer observed. Regarding the HAM and Efficientnet combination, the moderate correlation was mitigated toward a weak correlation.

## 6 Discussion

The nuances of the pigments, which had previously been neglected, were measured by the probability distribution with statistical distance. The results of Bayesian regression exposed the existence of a bias that could not be detected by fairness between groups. It was demonstrated that the correlation between distance and performance was mitigated by the loss function, which re-weighted the difference in skin color as a penalty. The starting epoch

Table 3: Results of correlation between skin nuance and F1-score and Accuracy

Dataset	Model	Prior Training		Posterior Training		Changes	
		F1-score	Accuracy	F1-score	Accuracy	F1-score	Accuracy
UTKFace	EffNet	-0.455	-0.319	-0.379	-0.209	0.076	0.110
	ResNet	-0.442	-0.316	-0.407	-0.257	0.035	0.059
	VGG	-0.448	-0.268	-0.430	-0.259	0.018	0.009
CelebA	EffNet	0.265	0.109	0.244	0.086	0.021	0.023
	ResNet	0.115	-0.084	0.111	-0.084	0.004	0.000
	VGG	0.156	0.040	0.150	-0.029	0.006	0.011
HAM	EffNet	-0.513	-0.555	-0.412	-0.329	0.101	0.226
	ResNet	-0.629	-0.424	-0.533	-0.355	0.096	0.069
	VGG	-0.497	-0.377	-0.600	-0.425	-0.103	0.048

to apply the penalty differs depending on the combination of the model and dataset. In this experiment, most combinations succeeded by beginning about 30% of the total training epochs for most combinations. Although Sample 3 in Figure 3 is a monochrome image, it has been annotated by human intuition and classified as ‘white’. However, when observing the color alone, it is apparent that it differs from other ‘white’ skin tones, highlighting the limitations of relying solely on human-assigned labels. This involves consideration beyond mere color perception. Distinctly, our approach focuses exclusively on the skin tone of the image being evaluated, which obviates the need for it to be supplemented by subjective assessments or other extrinsic factors. **This unique perspective has not been explored in prior research; therefore, a direct comparison with existing techniques is not feasible. This underscores the novelty of our method in addressing fairness in image classification by isolating and analyzing the inherent skin tone directly from the image data for the first time.**

### 6.1 Future work

There are two possible future tasks for this research. Although this manuscript focused on Wasserstein Distance, it is possible to reduce further performance differences due to individual skin color by investigating various statistical distance methods. The method can also be applicable to image-to-image generation and language-to-image models. The method allows us to evaluate the variation in the skin color range of the generated images.

### 6.2 Limitations

This proposal requires the identification of skin pixels. The detection of skin pixels relies on existing methods, such as publicly available segment images and landmarks. However, the skin detection mechanism is out of our research scope. It cannot be applied to datasets lacking skin detection methods, such as Fitzpatrick17K Groh et al. (2022, 2021) and Diverse Dermatology Images Daneshjou et al. (2022), in cases where there is no segment data, tiny skin areas, or skin lesions of multiple individuals in a single image.



## 7 Conclusion

The performance of models with different skin tones of individuals was assessed by measuring the gradation matrix that skin tones have using statistical distance measures and without categorizing skin types. The results demonstrated that biases latent within the same category could be detected. Moreover, by weighting the loss function according to nuanced differences in skin color, the correlation with the target evaluation metric was significantly reduced. In the future, this mechanism could be applied to generative models.

## Acknowledgments and Disclosure of Funding

The authors would like to thank the Dependable Intelligence Systems Lab, the Responsible AI Hull Research Group, and the Data Science, Artificial Intelligence, and Modelling (DAIM) Institute at the University of Hull for their support. Furthermore, the author extends heartfelt gratitude to Dr. Jun-ya Norimatsu at ALINEAR Corp. for technical advice with the experiments.

## References

- Teanna Barrett, Quanze Chen, and Amy Zhang. Skin deep: Investigating subjectivity in skin tone annotations for computer vision benchmark datasets. In *Proceedings of the 2023 ACM Conference on Fairness, Accountability, and Transparency*, pages 1757–1771, 2023.
- Peter J Bevan and Amir Atapour-Abarghouei. Detecting melanoma fairly: Skin tone detection and debiasing for skin lesion classification. In *MICCAI Workshop on Domain Adaptation and Representation Transfer*, pages 1–11. Springer, 2022.
- Reuben Binns. On the apparent conflict between individual and group fairness. In *Proceedings of the 2020 conference on fairness, accountability, and transparency*, pages 514–524, 2020.
- Renan DB Brotto, Jean-Michel Loubes, Laurent Risser, Jean-Pierre Florens, Kenji Nose-Filho, and João MT Romano. Debiasing machine learning models by using weakly supervised learning. *arXiv preprint arXiv:2402.15477*, 2024.
- Rodolfo A Bulatao and Norman B Anderson. Understanding racial and ethnic differences in health in late life: A research agenda. *Understanding Racial and Ethnic Differences in Health in Late Life*, 2004.
- Joy Buolamwini and Timnit Gebru. Gender shades: Intersectional accuracy disparities in commercial gender classification. In *Conference on fairness, accountability and transparency*, pages 77–91. PMLR, 2018.
- Yuhang Cai and Lek-Heng Lim. Distances between probability distributions of different dimensions. *IEEE Transactions on Information Theory*, 68(6):4020–4031, 2022.
- Silvia Chiappa and Aldo Pacchiano. Fairness with continuous optimal transport. *arXiv preprint arXiv:2101.02084*, 2021.

- Ching-Hao Chiu, Yu-Jen Chen, Yawen Wu, Yiyu Shi, and Tsung-Yi Ho. Achieve fairness without demographics for dermatological disease diagnosis. *Medical Image Analysis*, 95: 103188, 2024.
- Alexandra Chouldechova and Aaron Roth. The frontiers of fairness in machine learning. *arXiv preprint arXiv:1810.08810*, 2018.
- Adam Corbin and Oge Marques. Exploring strategies to generate fitzpatrick skin type metadata for dermoscopic images using individual typology angle techniques. *Multimedia Tools and Applications*, 82(15):23771–23795, 2023.
- Roxana Daneshjou, Kailas Vodrahalli, Roberto A Novoa, Melissa Jenkins, Weixin Liang, Veronica Rotemberg, Justin Ko, Susan M Swetter, Elizabeth E Bailey, Olivier Gevaert, et al. Disparities in dermatology ai performance on a diverse, curated clinical image set. *Science advances*, 8(31):eabq6147, 2022.
- Saloni Dash, Vineeth N Balasubramanian, and Amit Sharma. Evaluating and mitigating bias in image classifiers: A causal perspective using counterfactuals. In *Proceedings of the IEEE/CVF Winter Conference on Applications of Computer Vision*, pages 915–924, 2022.
- Siyi Du, Ben Hers, Nourhan Bayasi, Ghassan Hamarneh, and Rafeef Garbi. Fairdisco: Fairer ai in dermatology via disentanglement contrastive learning. In *European Conference on Computer Vision*, pages 185–202. Springer, 2022.
- Cynthia Dwork, Moritz Hardt, Toniann Pitassi, Omer Reingold, and Richard Zemel. Fairness through awareness. In *Proceedings of the 3rd innovations in theoretical computer science conference*, pages 214–226, 2012.
- Thomas B Fitzpatrick. The validity and practicality of sun-reactive skin types i through vi. *Archives of dermatology*, 124(6):869–871, 1988.
- Hemanth Gaddey, Vidhi Mittal, Manisha Chawla, Gagan Raj Gupta, et al. Patchalign: Fair and accurate skin disease image classification by alignment with clinical labels. *arXiv preprint arXiv:2409.04975*, 2024.
- Luca Giuliani, Eleonora Misino, and Michele Lombardi. Generalized disparate impact for configurable fairness solutions in ml. In *International Conference on Machine Learning*, pages 11443–11458. PMLR, 2023.
- Vincent Grari, Boris Ruf, Sylvain Lamprier, and Marcin Detyniecki. Fairness-aware neural r\’eyni minimization for continuous features. *arXiv preprint arXiv:1911.04929*, 2019.
- Matthew Groh, Caleb Harris, Luis Soenksen, Felix Lau, Rachel Han, Aerin Kim, Arash Koochek, and Omar Badri. Evaluating deep neural networks trained on clinical images in dermatology with the fitzpatrick 17k dataset. In *Proceedings of the IEEE/CVF Conference on Computer Vision and Pattern Recognition*, pages 1820–1828, 2021.

- Matthew Groh, Caleb Harris, Roxana Daneshjou, Omar Badri, and Arash Koochek. Towards transparency in dermatology image datasets with skin tone annotations by experts, crowds, and an algorithm. *Proceedings of the ACM on Human-Computer Interaction*, 6 (CSCW2):1–26, 2022.
- Laura Gustafson, Chloe Rolland, Nikhila Ravi, Quentin Duval, Aaron Adcock, Cheng-Yang Fu, Melissa Hall, and Candace Ross. Facet: Fairness in computer vision evaluation benchmark. In *Proceedings of the IEEE/CVF International Conference on Computer Vision*, pages 20370–20382, 2023.
- Tobias Hänel, Nishant Kumar, Dmitrij Schlesinger, Mengze Li, Erdem Ünal, Abouzar Es-lami, and Stefan Gumhold. Enhancing fairness of visual attribute predictors. In *Proceedings of the Asian conference on computer vision*, pages 1211–1227, 2022.
- Moritz Hardt, Eric Price, and Nati Srebro. Equality of opportunity in supervised learning. *Advances in neural information processing systems*, 29, 2016.
- Kaiming He, Xiangyu Zhang, Shaoqing Ren, and Jian Sun. Deep residual learning for image recognition. In *Proceedings of the IEEE conference on computer vision and pattern recognition*, pages 770–778, 2016.
- Courtney M Heldreth, Ellis P Monk, Alan T Clark, Candice Schumann, Xango Eyee, and Susanna Ricco. Which skin tone measures are the most inclusive? an investigation of skin tone measures for artificial intelligence. *ACM Journal on Responsible Computing*, 1 (1):1–21, 2024.
- Sunhee Hwang, Sungho Park, Pilhyeon Lee, Seogkyu Jeon, Dohyung Kim, and Hyeran Byun. Exploiting transferable knowledge for fairness-aware image classification. In *Proceedings of the Asian Conference on Computer Vision*, 2020.
- Abigail Z Jacobs and Hanna Wallach. Measurement and fairness. In *Proceedings of the 2021 ACM conference on fairness, accountability, and transparency*, pages 375–385, 2021.
- Joanna Jaworek-Korjakowska and Ryszard Tadeusiewicz. Hair removal from dermoscopic color images. *Bio-Algorithms and Med-Systems*, 9(2):53–58, 2013.
- Yan Ju, Shu Hu, Shan Jia, George H Chen, and Siwei Lyu. Improving fairness in deep-fake detection. In *Proceedings of the IEEE/CVF Winter Conference on Applications of Computer Vision*, pages 4655–4665, 2024.
- Thorsten Kalb, Kaiser Kushibar, Celia Cintas, Karim Lekadir, Oliver Diaz, and Richard Osuala. Revisiting skin tone fairness in dermatological lesion classification. In *Workshop on Clinical Image-Based Procedures*, pages 246–255. Springer, 2023.
- Kimmo Karkkainen and Jungseock Joo. Fairface: Face attribute dataset for balanced race, gender, and age for bias measurement and mitigation. In *Proceedings of the IEEE/CVF winter conference on applications of computer vision*, pages 1548–1558, 2021.
- Davis E. King. Dlib-ml: A machine learning toolkit. *Journal of Machine Learning Research*, 10:1755–1758, 2009.

- Newton M Kinyanjui, Timothy Odonga, Celia Cintas, Noel CF Codella, Rameswar Panda, Prasanna Sattigeri, and Kush R Varshney. Estimating skin tone and effects on classification performance in dermatology datasets. *arXiv preprint arXiv:1910.13268*, 2019.
- KS Krishnapriya, Michael C King, and Kevin W Bowyer. Analysis of manual and automated skin tone assignments for face recognition applications. *arXiv preprint arXiv:2104.14685*, 2021.
- Joshua Lee, Yuheng Bu, Prasanna Sattigeri, Rameswar Panda, Gregory Wornell, Leonid Karlinsky, and Rogerio Feris. A maximal correlation approach to imposing fairness in machine learning. In *ICASSP 2022-2022 IEEE International Conference on Acoustics, Speech and Signal Processing (ICASSP)*, pages 3523–3527. IEEE, 2022.
- Joshua K Lee, Yuheng Bu, Deepta Rajan, Prasanna Sattigeri, Rameswar Panda, Subhro Das, and Gregory W Wornell. Fair selective classification via sufficiency. In *International conference on machine learning*, pages 6076–6086. PMLR, 2021.
- Tim Lee, Vincent Ng, Richard Gallagher, Andrew Coldman, and David McLean. Dull-razor®: A software approach to hair removal from images. *Computers in biology and medicine*, 27(6):533–543, 1997.
- legislation.gov.uk. Equality act 2010, June 2013. URL <https://www.legislation.gov.uk/ukpga/2010/15/part/2/chapter/1>.
- Jiazhi Li and Wael Abd-Almageed. Cat: Controllable attribute translation for fair facial attribute classification. In *European Conference on Computer Vision*, pages 363–381. Springer, 2022.
- Xiaoxiao Li, Ziteng Cui, Yifan Wu, Lin Gu, and Tatsuya Harada. Estimating and improving fairness with adversarial learning. *arXiv preprint arXiv:2103.04243*, 2021.
- Li Lin, Xinan He, Yan Ju, Xin Wang, Feng Ding, and Shu Hu. Preserving fairness generalization in deepfake detection. In *Proceedings of the IEEE/CVF Conference on Computer Vision and Pattern Recognition*, pages 16815–16825, 2024.
- Xiaofeng Lin, Seungbae Kim, and Jungseock Joo. Fairgrape: Fairness-aware gradient pruning method for face attribute classification. In *European Conference on Computer Vision*, pages 414–432. Springer, 2022.
- Ziwei Liu, Ping Luo, Xiaogang Wang, and Xiaoou Tang. Deep learning face attributes in the wild. In *Proceedings of the IEEE international conference on computer vision*, pages 3730–3738, 2015.
- Ayesha Manzoor and Ajita Rattani. Fineface: Fair facial attribute classification leveraging fine-grained features. *arXiv preprint arXiv:2408.16881*, 2024.
- J  r  mie Mary, Cl  ment Calauzenes, and Nouredine El Karoui. Fairness-aware learning for continuous attributes and treatments. In *International Conference on Machine Learning*, pages 4382–4391. PMLR, 2019.

- Youssef Mohamed, Bilal Koussayer, Ellie M Randolph, William West III, Julia A Morris, Nicole K Le, Kristen Whalen, Kristina Gemayel, Mahmood J Al Bayati, Jared Troy, et al. A novel method to determine patient skin type: The skin analyzer. *Plastic and Reconstructive Surgery–Global Open*, 11(10):e5341, 2023.
- Vidya Muthukumar. Color-theoretic experiments to understand unequal gender classification accuracy from face images. In *Proceedings of the IEEE/CVF Conference on Computer Vision and Pattern Recognition Workshops*, pages 0–0, 2019.
- Luca Oneto, Michele Donini, and Massimiliano Pontil. General fair empirical risk minimization. In *2020 International Joint Conference on Neural Networks (IJCNN)*, pages 1–8. IEEE, 2020.
- Arezou Pakzad, Kumar Abhishek, and Ghassan Hamarneh. Circle: Color invariant representation learning for unbiased classification of skin lesions. In *European Conference on Computer Vision*, pages 203–219. Springer, 2022.
- Sungho Park, Bei Liu, Jianlong Fu, and Hyeran Byun. Unsupervised fairness-aware framework for image classification. *Available at SSRN 4496791*, 2022.
- Eman Rezk, Mohamed Eltorki, Wael El-Dakhakhni, et al. Improving skin color diversity in cancer detection: deep learning approach. *JMIR Dermatology*, 5(3):e39143, 2022.
- Salvatore Ruggieri, Jose M Alvarez, Andrea Pugnana, Franco Turini, et al. Can we trust fair-ai? In *Proceedings of the AAAI Conference on Artificial Intelligence*, pages 15421–15430, 2023.
- Ioannis Sarridis, Christos Koutlis, Symeon Papadopoulos, and Christos Diou. Towards fair face verification: An in-depth analysis of demographic biases. *arXiv preprint arXiv:2307.10011*, 2023.
- Candice Schumann, Femi Olanubi, Auriel Wright, Ellis Monk, Courtney Heldreth, and Susanna Ricco. Consensus and subjectivity of skin tone annotation for ml fairness. *Advances in Neural Information Processing Systems*, 36, 2024.
- Karen Simonyan and Andrew Zisserman. Very deep convolutional networks for large-scale image recognition. *arXiv preprint arXiv:1409.1556*, 2014.
- Çağrı Suiçmez, Hamdi Tolga Kahraman, Alihan Suiçmez, Cemal Yılmaz, and Furkan Balcı. Detection of melanoma with hybrid learning method by removing hair from dermoscopic images using image processing techniques and wavelet transform. *Biomedical Signal Processing and Control*, 84:104729, 2023.
- Mingxing Tan and Quoc Le. Efficientnet: Rethinking model scaling for convolutional neural networks. In *International conference on machine learning*, pages 6105–6114. PMLR, 2019.
- William Thong and Cees GM Snoek. Feature and label embedding spaces matter in addressing image classifier bias. *arXiv preprint arXiv:2110.14336*, 2021.

- William Thong, Przemyslaw Joniak, and Alice Xiang. Beyond skin tone: A multidimensional measure of apparent skin color. In *Proceedings of the IEEE/CVF International Conference on Computer Vision*, pages 4903–4913, 2023.
- Huan Tian, Tianqing Zhu, Wei Liu, and Wanlei Zhou. Image fairness in deep learning: problems, models, and challenges. *Neural Computing and Applications*, 34(15):12875–12893, 2022.
- Philipp Tschandl, Cliff Rosendahl, and Harald Kittler. The ham10000 dataset, a large collection of multi-source dermatoscopic images of common pigmented skin lesions. *scientific data*. 2018; 5: 180161. *Search in*, 2, 2018.
- Philipp Tschandl, Christoph Rinner, Zoe Apalla, Giuseppe Argenziano, Noel Codella, Allan Halpern, Monika Janda, Aimilios Lallas, Caterina Longo, Josep Malvehy, et al. Human–computer collaboration for skin cancer recognition. *Nature Medicine*, 26(8):1229–1234, 2020.
- Mei Wang and Weihong Deng. Mitigating bias in face recognition using skewness-aware reinforcement learning. In *Proceedings of the IEEE/CVF conference on computer vision and pattern recognition*, pages 9322–9331, 2020.
- Zhibo Wang, Xiaowei Dong, Henry Xue, Zhifei Zhang, Weifeng Chiu, Tao Wei, and Kui Ren. Fairness-aware adversarial perturbation towards bias mitigation for deployed deep models. In *Proceedings of the IEEE/CVF conference on computer vision and pattern recognition*, pages 10379–10388, 2022.
- Yawen Wu, Dewen Zeng, Xiaowei Xu, Yiyu Shi, and Jingtong Hu. Fairprune: Achieving fairness through pruning for dermatological disease diagnosis. In *International Conference on Medical Image Computing and Computer-Assisted Intervention*, pages 743–753. Springer, 2022.
- Alice Xiang and Inioluwa Deborah Raji. On the legal compatibility of fairness definitions. *arXiv preprint arXiv:1912.00761*, 2019.
- Ruichen Yao, Ziteng Cui, Xiaoxiao Li, and Lin Gu. Improving fairness in image classification via sketching. *arXiv preprint arXiv:2211.00168*, 2022.
- Haolin Yuan, Armin Hadzic, William Paul, Daniella Villegas de Flores, Philip Mathew, John Aucott, Yinzhi Cao, and Philippe Burlina. Edgemixup: improving fairness for skin disease classification and segmentation. *arXiv preprint arXiv:2202.13883*, 2022.
- Muhammad Bilal Zafar, Isabel Valera, Manuel Gomez Rrogriguez, and Krishna P Gummadi. Fairness constraints: Mechanisms for fair classification. In *Artificial intelligence and statistics*, pages 962–970. PMLR, 2017.
- Guanhua Zhang, Yihua Zhang, Yang Zhang, Wenqi Fan, Qing Li, Sijia Liu, and Shiyu Chang. Fairness reprogramming. *Advances in Neural Information Processing Systems*, 35:34347–34362, 2022.

Zhifei Zhang, Yang Song, and Hairong Qi. Age progression/regression by conditional adversarial autoencoder. In *Proceedings of the IEEE conference on computer vision and pattern recognition*, pages 5810–5818, 2017.

## Appendix A. Prior Training Model Performance

This Table 4 provides the performance results of a generic model with a commonly assessed group fairness. In this research, the model was employed for the purpose of Bayesian regression prior distributions.

Table 4: Experiment models and the general performance

Dataset	UTKFace			CelebA			HAM		
Model	EffNet	ResNet	VGG	EffNet	ResNet	VGG	EffNet	ResNet	VGG
lr	1e-5	1e-5	1e-6	1e-6	1e-6	1e-6	1e-5	1e-6	1e-6
Epochs	14	17	24	29	28	24	18	23	33
Val F1	0.92	0.90	0.88	0.91	0.88	0.91	0.89	0.80	0.83
Val ACC	0.92	0.90	0.88	0.91	0.88	0.91	0.89	0.80	0.83
Test F1	0.91	0.90	0.88	0.91	0.87	0.90	0.88	0.78	0.82
Test ACC	0.91	0.90	0.88	0.91	0.87	0.90	0.88	0.78	0.82

## Appendix B. Equal Odds, Demographic Parity for Continuous Sensitive Attributes Using Wasserstein Distance

In this appendix, we extend the traditional Equal Opportunity fairness constraint to accommodate continuous sensitive attributes by incorporating the Wasserstein Distance (WD). Specifically, we address the challenge of applying fairness metrics to a continuous attribute such as skin tone, where traditional binary or categorical approaches are insufficient.

### B.1 Demographic Parity

#### B.1.1 BACKGROUND

Demographic Parity (DP) Zafar et al. (2017) is a fairness criterion that requires the predicted outcome  $\hat{Y}$  to be independent of the sensitive attribute  $A$ . For a binary sensitive attribute, DP is defined as:

$$P(\hat{Y} = 1 \mid A = 0) = P(\hat{Y} = 1 \mid A = 1). \quad (11)$$

#### B.1.2 EXTENSION TO CONTINUOUS SENSITIVE ATTRIBUTES

When  $A$  is continuous, Equation (11) is not directly applicable. To extend DP to continuous  $A$ , we utilize the Wasserstein Distance to measure the difference between different values of  $A$  and a reference point  $A_0$  (e.g., the lightest skin tone).

#### B.1.3 WASSERSTEIN DISTANCE WITH DIRECTIONAL SIGNIFICANCE

Let  $\mathcal{F}(A)$  denote the cumulative distribution function (CDF) of the sensitive attribute  $A$ . The Wasserstein Distance between two values  $A_0$  and  $A$  is defined as:

$$\mathcal{D}(A_0, A) = \int_{A_0}^A |\mathcal{F}(a) - \mathcal{F}(A_0)| da \cdot \text{sign}(A - A_0), \quad (12)$$



where  $\text{sign}(A - A_0)$  captures the direction of the difference.

#### B.1.4 REWRITING THE DEMOGRAPHIC PARITY CONSTRAINT

We adjust the Demographic Parity constraint to incorporate the continuous nature of  $A$  and the distance metric:

$$\int_{-\infty}^{\infty} \mathcal{D}(A_0, A) \left[ P(\hat{Y} = 1 | A) - P(\hat{Y} = 1 | A_0) \right] dF_A(A) = 0. \quad (13)$$

where  $dF_A(A)$  is the probability density function of  $A$ .

#### B.1.5 INTERPRETATION

Equation (13) ensures that the weighted differences in the probability of a positive prediction between any value of  $A$  and the reference point  $A_0$  integrate to zero over the distribution of  $A$ . The weighting by  $\mathcal{D}(A_0, A)$  accounts for both the magnitude and direction of the differences in the sensitive attribute.

### B.2 Equalized Odds

#### B.2.1 BACKGROUND

Equalized Odds (EO) Hardt et al. (2016) requires that both the true positive rates (TPR) and false positive rates (FPR) are equal across groups defined by the sensitive attribute  $A$ . For a binary-sensitive attribute, EO is expressed as:

$$P(\hat{Y} = 1 | A = 0, Y = y) = P(\hat{Y} = 1 | A = 1, Y = y), \text{ for } y \in \{0, 1\}. \quad (14)$$

#### B.2.2 EXTENSION TO CONTINUOUS SENSITIVE ATTRIBUTES

To extend EO to a continuous  $A$ , we again incorporate the Wasserstein Distance to account for differences across the continuous domain.

#### B.2.3 REWRITING THE EQUAL ODDS CONSTRAINT

The adjusted EO constraint is given by:

$$\int_{-\infty}^{\infty} \mathcal{D}(A_0, A) [P(\hat{Y} = 1 | A, Y = y) - P(\hat{Y} = 1 | A_0, Y = y)] dF_{A|Y=y}(A) = 0, \quad \text{for } y \in \{0, 1\}, \quad (15)$$

where  $dF_{A|Y=y}(A)$  is the conditional probability density function of  $A$  given  $Y = y$ .

#### B.2.4 INTERPRETATION

Equation (15) ensures that the weighted differences in prediction probabilities between any value of  $A$  and the reference point  $A_0$ , conditioned on the true label  $Y = y$ , integrate to zero over the distribution of  $A$  given  $Y = y$ . This enforces that both TPR and FPR are balanced across the spectrum of the sensitive attribute.

### B.3 Implications

These formulations generalize the Equal Opportunity, Demographic Parity and Equalized Odds criteria to continuous sensitive attributes by:

- Utilizing the Wasserstein Distance to quantify differences across the continuous domain of  $A$ .
- Incorporating the sign function to maintain the directional significance of these differences.
- Ensuring fairness by balancing the weighted disparities in prediction probabilities across all values of  $A$ .

### Appendix C. Source code

The source code we created for the experiment is available here [this GitHub repository](#).